HHS Public Access

Author manuscript

J Invest Dermatol. Author manuscript; available in PMC 2013 October 01.

Published in final edited form as:

J Invest Dermatol. 2013 April ; 133(4): 1088–1096. doi:10.1038/jid.2012.410.

A synthetic superoxide dismutase/catalase mimetic EUK-207 mitigates radiation dermatitis and promotes wound healing in irradiated rat skin

Susan R. Doctrow[2,*], **Argelia Lopez**[1,*], **Ashley M. Schock**[1], **Nathan E. Duncan**[1], **Megan M. Jourdan**[1], **Edit B. Olasz**[1], **John E. Moulder**[3], **Brian L. Fish**[3], **Marylou Mäder**[3], **Jozef Lazar**[1], and **Zelmira Lazarova**[1]

[1]Department of Dermatology, Boston University School of Medicine, Boston, MA, USA

[2]Department of Medicine, Boston University School of Medicine, Boston, MA, USA

[3]Department of Radiation Oncology Center for Medical Countermeasures against Radiological Terrorism, Medical College of Wisconsin, Milwaukee, Wisconsin, and Pulmonary Center, Boston University School of Medicine, Boston, MA, USA

Abstract

In the event of a radionuclear attack or nuclear accident, the skin would be the first barrier exposed to radiation, though skin injury can progress over days to years following exposure. Chronic oxidative stress has been implicated as being a potential contributor to the progression of delayed radiation-induced injury to skin and other organs. To examine the causative role of oxidative stress in delayed radiation-induced skin injury, including impaired wound healing, we tested a synthetic superoxide dismutase (SOD)/catalase mimetic, EUK-207, in a rat model of combined skin irradiation and wound injury. Administered systemically, beginning 48 h after irradiation, EUK-207 mitigated radiation dermatitis, suppressed indicators of tissue oxidative stress, and enhanced wound healing. Evaluation of gene expression in irradiated skin at 30 days after exposure revealed a significant upregulation of several key genes involved in detoxication of reactive oxygen and nitrogen species. This gene expression pattern was primarily reversed by EUK-207 therapy. These results demonstrate that oxidative stress plays a critical role in the progression of radiation-induced skin injury, and that the injury can be mitigated by appropriate antioxidant compounds administered 48 h after exposure.

Keywords

EUK-207; radiation dermatitis; oxidative stress; wound healing

Corresponding author: Zelmira Lazarova, MD, Department of Dermatology, Medical College of Wisconsin, 8701 Watertown Plank Road, Milwaukee, WI 53226-4801, Telephone: 414-955 4061, zlazarov@mcw.edu.

*These authors contributed equally on this work.

Conflict of Interest: The authors state no conflict of interest. Dr. Doctrow is an inventor of patents describing EUK-207 and other salen Mn complexes, developed while she was employed at Eukarion, Inc. However, the company is no longer in business and she has retained no stock options or other rights.

INTRODUCTION

Cutaneous radiation syndrome (CRS) may occur after total or partial body exposure to gamma radiation which penetrates deep into underlying tissue. It can also result from exposure to high-energy beta radiation which usually does not penetrate sufficiently deep to cause hematopoietic, gastrointestinal or neurovascular injury. CRS is an important concern for subjects exposed during a radiological accident or terrorist attack (Peter, 2005). Experience following the Chernobyl nuclear plant accident showed the impact of skin injury on patient prognosis. Almost half of the exposed individuals suffered from CRS and nearly 50% of these died with primary cause of death attributed to CRS (Mettler *et al.*, 2007). Moreover, radiation dermatitis is a common consequence of radiation cancer therapy, and can be followed months later with atrophy, fibrosis, or telangiectasia (Ryan, 2012). It is well documented that cutaneous radiation exposure impairs wound healing (Jourdan *et al.*; Liu *et al.*, 2005; Riedel *et al.*, 2005; Schwentker *et al.*, 1998; Wang *et al.*, 2006).

Growing evidence links oxidative stress to the skin injury following acute radiation exposure (Robbins and Zhao, 2004; Zhao *et al.*, 2007). We addressed the hypothesis that an antioxidant compound with appropriate properties would show benefits in both acute and chronic models of cutaneous radiation injury. We employed EUK-207, one of a class of synthetic compounds, salen Mn complexes, that mimic the antioxidant enzymes SOD and catalase, scavenging the reactive oxygen species (ROS) superoxide, O^{2-}, and hydrogen peroxide, H_2O_2 (Doctrow *et al.*, 2005; Doctrow *et al.*, 2002), and reactive nitrogen species (Sharpe *et al.*, 2002). Consistent with their catalase activity, salen Mn complexes are peroxidase mimetics (Doctrow *et al.*, 2002), further broadening their potential to scavenge hydroperoxides and otherwise modulate the cellular redox environment. Such properties confer advantages over other antioxidants, such as noncatalytic or protein-based agents (Doctrow, 2003; Doctrow *et al.*, 1997).

Prototype salen Mn complexes EUK-8, EUK-134 and EUK-189 are cytoprotective in various experimental systems (Doctrow *et al.*, 2005; Doctrow *et al.*, 2002; Halliwell and Gutteridge, 2007). EUK-207 is a newer generation cyclized salen Mn complex that has catalytic properties equivalent to those of EUK-134 and EUK-189, but greater stability and *in vivo* half-life (Doctrow *et al.*, 2005; Liu *et al.*, 2003; Rosenthal *et al.*, 2011). The structure of EUK-207, with Mn bound to a poly-ether cyclized salen ligand, has been previously reported (Rosenthal *et al*., 2009; Liu *et al*., 2003). EUK-207 mitigates delayed radiation injury to the lung (Gao *et al.*, 2012; Mahmood *et al.*, 2011; Rosenthal *et al.*, 2011) and kidney (Rosenthal *et al.*, 2011) in rats, protects murine hearts from cardiac ischemia-reperfusion (Liesa *et al.*, 2011), and improves age-associated cognitive impairment in mice (Clausen *et al.*, 2010; Liu *et al.*, 2003). In many of these efficacy models, salen Mn complexes are not only functionally protective, but also suppress oxidative modifications of proteins, lipids and nucleic acids (Clausen *et al.*, 2010; Gonzalez *et al.*, 1995; Jung *et al.*, 2001; Liesa *et al.*, 2011; Liu *et al.*, 2003; Mahmood *et al.*, 2011; Rong *et al.*, 1999; Zhang *et al.*, 2004). Salen Mn complexes are of further interest, as compared to other synthetic antioxidants, because of their "mitoprotective" properties in experimental models for mitochondrial injury (Doctrow *et al.*, 2012; Doctrow *et al.*, 2005; Liesa *et al.*, 2011; Melov *et al.*, 2001; Rosenthal *et al.*, 2011).

We developed an animal model of combined radiation and wound injury to the skin where radiation-induced skin injury affected approximately 10% of total body surface, radiation did not penetrate deep into the tissues, and radiation exposure was accompanied by two full-thickness skin wounds (Jourdan *et al.*, 2011). Rats treated under this combined injury protocol developed, in a radiation dose-dependent manner, acute radiation dermatitis spanning in severity from transient erythema to non-healing ulcers, as well as markedly impaired wound healing. Using this model, EUK-207 was tested as a potential mitigating drug on endpoints relevant to radiation dermatitis, skin wound healing, and chronic oxidative stress.

RESULTS

EUK-207 mitigates radiation dermatitis

For this study, we employed a 30 Gy radiation dose that, without drug treatment, induced severe radiation dermatitis within 17–21 days after irradiation and ulcers that failed to heal over the 90 day observation period (Jourdan *et al.*, 2011). Unanesthetized rats (n=48) were randomly divided into two experimental groups, irradiated, and given whole thickness wounds as described in Methods. Control animals (n=14) were sham irradiated, and wounded in the same manner. EUK-207 (1.8 mg/kg-day) or vehicle (water) was given by subcutaneous infusion beginning 48 hours after irradiation and continuing for up to 90 days. This delayed time was selected because, in a mass casualty scenario, therapies might be unavailable until long after radiation exposure. Radiation dermatitis was scored weekly as described in Methods.

The EUK-207-treated group showed reduced radiation dermatitis severity by 30 days post-irradiation (Figure 1a, 1b). Skin injury scores continued to improve, remaining significantly lower than in vehicle-treated rats ($p<0.01$; Figure 1b). At 90 days after irradiation, EUK-207-treated rats had only mild alopecia with multiple hairs growing in the center of radiation field. In contrast, vehicle-treated rats had permanent alopecia, persistent erythema, and non-healing ulcers (Figure 1b).

EUK-207 improves wound healing and histological structure of irradiated skin

At 21 days after wounding, EUK-207 treated rats showed significantly smaller wounds than vehicle-treated (32% versus 58% of original wound size; $p<0.05$) (Figure 2a). Wounds in the EUK-207 treated group became completely healed within 35±4 days (data not shown). This is in contrast to the wounds in the vehicle-treated group which, like those in the originally-described model (Jourdan *et al.*, 2011), did not fully heal during the duration of the study.

Since new blood vessels are an integral part of granulation tissue needed for the wound healing process, we evaluated blood vessel density as described in Methods. The number of blood vessels per optical field was decreased in irradiated skin, as early as 7 days following irradiation, as compared to in non-irradiated control animals (9.8±2.9 vs. 25.3±4.6; $p<0.0001$). The lower blood vessel density remained at the 14 day time point (9.4±3.7), and was further declined (3.3±2.3) at 30 days after irradiation. The blood vessel density in tissue

samples taken from the wound edge 30 days after irradiation were dramatically increased with EUK-207 treatment (29.8±14.3 vs. 3.3±2.3; p<0.006) (Figure 2b and 2c).

Based on several histological indicators, the skin in the EUK-207 treated group displayed reduced injury and a more normalized phenotype (Figure 3a). These included reduction of dermal thickness at 30 and 90 days (p<0.005), increased epidermal thickness at 30 days (p<0.005), and restoration of hair growth signified by increased number of hair follicles (p<0.03; Figure 3b).

EUK-207 normalizes the gene expression pattern in irradiated skin

Chronic oxidative stress has been implicated in the progression of radiation-induced late effects, potentially via activation or repression of genes in important signaling pathways, but the specific genes involved in radiation-induced skin injury are ill-defined. We therefore obtained gene expression data on skin samples taken 30 days after irradiation. To evaluate gene expression patterns relevant to oxidative stress, mRNA was prepared from unirradiated and irradiated (control and EUK-207 treated) rats and analyzed by microarray as described in Methods. The data indicated that irradiation caused upregulation of 15 genes, including those involved in generation or detoxification of ROS, and downregulation of genes involved in excisional DNA repair (Xpa) or innate immunity (Mpo) (Table 1a). These changes were abrogated in skin from irradiated rats receiving EUK-207. In these rats, there was up-regulation of only three genes from the oxidative stress pathway, all changes distinct from those in the vehicletreated group (Table 1b).

EUK-207 reduces oxidation of proteins and nucleic acids

Since the gene expression data demonstrated radiation-induced dysregulation of genes responsive to oxidative stress, we examined oxidative modifications of proteins and nucleic acids to confirm the occurrence of chronic oxidative stress in irradiated skin. Protein carbonylation is a commonly used biomarker of irreversible oxidative damage to proteins (Levine, 2002). Skin extracts from the irradiated rats showed increased protein carbonyls at 30 and 90 days after irradiation, with one prominent band (MW ~68Kd) likely corresponding to albumin, which, due to abundance, frequently appears as a major carbonylated band (Levine *et al.*, 1994; Wehr and Levine, 2012). The cumulative density of all carbonylated bands was significantly attenuated by EUK-207 treatment (p<0.05*;* Figure 4a and 4b). Along with chronic oxidative damage to proteins, skin from irradiated rats also exhibited evidence for nucleic acid injury. Staining for oxidized 8-hydroxyguanosine (8-OHdG), a marker for DNA oxidation, was evident in irradiated skin even at 90 days after irradiation, and substantially decreased with EUK-207 treatment (Figure 4c and 4d).

DISCUSSION

It is well known that irradiation causes the immediate generation of short-lived ROS, but the role of chronically generated ROS in longer-term damage, though hypothesized and increasingly implicated (Zhao *et al.*, 2007; Zhao and Robbins, 2009), is not well documented. Our study demonstrates that chronic oxidative stress occurs in irradiated skin, even a month or more after exposure. Furthermore, the dramatic reduction of skin injury by

a synthetic SOD/catalase mimetic, EUK-207, concomitant with its abrogation of oxidative stress indicators, demonstrates that oxidative stress is causative in both chronic radiation dermatitis and impaired wound healing in irradiated skin. Because EUK-207 was initiated 48 hours after exposure, there is no question that the ROS targeted in our study are those generated well after the initial radiation insult. Increased localized expression of known antioxidant proteins was shown to decrease cutaneous radiation injury (Yan *et al.*, 2008; Zhang *et al.*, 2012). We further demonstrate, through mitigation by a synthetic antioxidant agent, that oxidative stress causes both the dermatitis and wound healing impairments characteristic of delayed radiation injury. Possibly, previously tested antioxidants either lacked the appropriate ROS specificity, did not have adequate bioavailability to the skin, or both. The required bioavailability may include access to the mitochondria, since mitochondrial dysfunction has been implicated in cellular sensitivity to radiation injury (Aykin-Burns *et al.*, 2011; Greenberger and Epperly, 2004; Jiang *et al.*, 2009). While we have not directly tested the role of "mito-protection" in this study, salen Mn complexes suppress oxidative mitochondrial injury in other experimental models (Doctrow *et al.*, 2012; Doctrow *et al.*, 2005; Liesa *et al.*, 2011; Melov *et al.*, 2001). Among the oxidative-stress responsive genes we found to be upregulated in irradiated, vehicle-treated skin is Sod2, for the mitochondrial antioxidant enzyme MnSOD (Table 1a). Sod2 is also upregulated in other models for radiation exposure, and increased SOD expression in the mitochondria is radioprotective (Epperly *et al.*, 2007; Greenberger and Epperly, 2007; Wong *et al.*, 1996). Our data also showed upregulation of genes for glutathione peroxidase 1 (Gpx1) and peroxidredoxin 5 (Prdx5). Peroxidredoxin 5 has been found in the mitochondria and is regarded as a potentially important scavenger of mitochondrial ROS, particularly hydroperoxides (Cox *et al.*, 2010) Glutathione peroxidase 1, a cytosolic enzyme, has been reported to play a role in modulating the mitochondria, through redox changes, and its upregulation has been implicated in mitochondrial dysfunction (Handy *et al.*, 2009). Overall, an upregulation of such mitochondrially associated antioxidant enzymes is potentially indicative of oxidative mitochondrial injury. If so, then prevention of their up regulation by EUK-207 (Table 1b) is consistent with a hypothesis that the compound's mitigating effects on cutaneous radiation injury are, at least in part, related to its ability to protect the mitochondria. However, its suppression of nearly all the changes in oxidative-stress responsive genes in irradiated skin indicates that EUK-207 is not acting exclusively at the mitochondria. This agrees with previous reports showing suppression of both mitochondrial (Hinerfeld *et al.*, 2004; Liesa *et al.*, 2011; Liu *et al.*, 2003; Melov *et al.*, 2001) and non-mitochondrial (Liesa *et al.*, 2011; Peng *et al.*, 2005; Rong *et al.*, 1999; Zhang *et al.*, 2004) oxidative modifications by salen Mn complexes. Indeed, unlike MitoQ and certain other antioxidants (Demianenko *et al.*, 2010; Murphy and Smith, 2007), the salen Mn complexes were not designed for specific mitochondrial targeting. It is interesting to note that, in the irradiated rat skin, the gene for glutathione peroxidase 2 (Gpx2) was downregulated with vehicle, yet upregulated with EUK-207 treatment. The significance of this reversal in Gpx2 expression by EUK-207 is not yet apparent, but should be studied further. While there is little literature to address its potential role in radiation injury or wound healing, glutathione peroxidase 2 has been reported to have both a cytoplasmic and mitochondrial location in yeast (Ukai *et al.*, 2011). In a recent study using diabetic mice (Tie *et al.*, 2012), GI-PS, a polysaccharide derived from the medicinal fungi Ganoderma lucidum, accelerated wound

healing while increasing total glutathione peroxidase activity in the skin. This enzymatic activity, of course, likely represents a combination of glutathione peroxidase 1, 2 and perhaps other forms. The GI-PS also increased skin MnSOD activity, not by changing the protein's expression but, instead, by suppressing its nitration, a known mechanism of its inactivation during oxidative stress. Based on the latter finding, Tie *et al*. attributed the wound healing properties of GI-PS to its known antioxidant properties and, in particular, to an inhibition of mitochondrial oxidative stress. In our study, it is also of interest that EUK-207 appeared to upregulate expression of peroxidredoxin 6 (Prdx6). Studies with Prdx6 knockout mice have indicated that peroxiredoxin 6 is essential for blood vessel integrity during skin wound healing, with vascular endothelial cells appearing to be highly sensitive to the loss of this novel peroxiredoxin (Kumin *et al*., 2006). Thus, in our model, the ability of EUK-207 to increase Prdx6 expression may relate to the compound's beneficial effects on wound healing and angiogenesis. From our perspective, these changes in gene expression are of interest as preliminary leads for future study, including a more detailed analysis of whether EUK-207 modulates protein levels or enzymatic activities of any of these potentially key antioxidant proteins during wound healing in irradiated skin.

Based on its other reported *in vivo* effects in radiation injury models (Mahmood *et al.*, 2011; Rosenthal *et al.*, 2011), mitigation of radiation dermatitis severity by EUK-207 was not unexpected. However, improved wound healing by an ROS scavenger was not necessarily predicted from literature describing a very complex association between ROS and normal skin wound healing. ROS, particularly H_2O_2, are believed to play key signaling roles to promote wound healing, and localized transfection of catalase delays healing in rodents (Roy *et al.*, 2006; Sen and Roy, 2008). Yet, excess H_2O_2 impairs (Roy *et al.*, 2006) and transfection with Sod2 improves wound healing (Luo *et al.*, 2004), as does chronic administration of a mitochondrially-targeted antioxidant (Demianenko *et al.*, 2010). Our observation that EUK-207 treatment resulted in increased angiogenesis in the irradiated wounded skin is particularly intriguing. ROS are believed to mediate mitogenesis stimulated by growth factors including the angiogenic factor VEGF (Roy *et al.*, 2006; Ushio-Fukai and Alexander, 2004). And, interestingly, an endogenously generated oxidized lipid product promotes angiogenesis and wound healing in a VEGF-independent manner (West *et al.*, 2010). Thus, one might expect an antioxidant to impair rather than, as we observe, facilitate angiogenesis. It is conceivable that, in our combined injury model, by promoting a more normalized skin phenotype (*e.g.* Figures 1 and 3), EUK-207 is inducing a microenvironment that facilitates more normal wound healing, enabling tissue remodeling processes including new blood vessel growth (Gurtner *et al.*, 2008). In support of this, the basement membrane deposition of laminin 332 is impaired in our model (Jourdan *et al.*, 2011) and is improved with EUK-207 treatment (data not shown). More broadly, EUK-207 may modify the microenvironment through suppression of oxidation-dependent events that might otherwise destroy microvasculature in irradiated tissue. Consistent with this, EUK-207 treatment preserves the microvasculature after lung irradiation (Gao *et al.*, 2012). Thus, overall, the role of ROS, particularly H_2O_2, and of redox regulation in cutaneous wound healing and its associated angiogenesis is highly complex. Despite this complexity, our study supports the concept that selected ROS-scavenging agents such as EUK-207, having the appropriate

specificity and given under the right circumstances, can mitigate radiation-induced skin injury, including facilitating wound healing.

MATERIALS AND METHODS

Animals

Sixty two syngeneic male WAG/RijCmcr eight-week-old rats bred and housed in a moderate-security barrier were used for this study. Rats were monitored daily and maintained on a 12-hours light/dark cycle, with free food and water intake. At the times specified below, animals were euthanized using isoflurane inhalation. All animal research was approved by the Medical College of Wisconsin Institutional Animal Care and Use Committee.

Irradiation and wounding protocol

We employed our previously published protocol (Jourdan *et al.*, 2011). Unanesthetized rats were immobilized and irradiated with an x-ray beam with a steep dose gradient in the dorso-ventral direction (without injury to the internal organs). The source-to-skin distance was 37 mm and the dose rate was 0.68 Gy per minute. The irradiated area of skin corresponded to 10% of the total body surface. Animals were randomly divided into two experimental groups and either sham irradiated (n=14) or irradiated with a single dose of 30 Gy defined at the dermal layer (n=48). Within one hour following irradiation, all rats were anesthetized, and two full-thickness wounds were made on the back of each rat within the irradiation field using an 8 mm punch biopsy. The wounds were left uncovered and animals were housed individually to prevent damage to the wound site.

Implantation of osmotic pumps for drug delivery

The custom synthesized EUK-207, (Liesa *et al.*, 2011) was dissolved in ultrapure water, filter-sterilized and administered by subcutaneous Alzet infusion pumps (DURECT Corporation, Cupertino, CA) at 1.8 mg/kg/day beginning 48 hours after irradiation and continuing for up to 90 days. Sham-irradiated or irradiated-only animals received pumps filled with vehicle. The EUK-207 dose was about 4-fold lower than doses employed previously to mitigate radiation injury to rat lung (Mahmood *et al*., 2011) and kidney (Rosenthal *et al*., 2011). This lower dose was selected to eliminate the localized skin toxicities observed in those prior studies, while remaining well within the effective EUK-207 dose range reported in other rodent models (e.g. Liu *et al*., 2003).

Monitoring of radiation dermatitis and wound closure

Photographs of animals were taken three times per week and coded. The skin injury score was assessed from coded images by two investigators in a masked fashion according to a previously published scoring system (Jourdan *et al*., 2011). Wound contraction was assessed at days 0, 3, 7, 14 and 21. Wound areas were not calculated at later time points due to heavy crusts covering the wounds and multiple erosions blending into the wound site. Wound area was determined as described (Jourdan *et al*., 2011) and wound contraction was calculated as follows:

$$\text{Percentage wound contraction on } N^{th}\text{day} = 100 - \left(\frac{\text{wound area on } N^{th}\text{day}}{\text{wound area on } 1^{st}\text{day}}\right) \times 100$$

Skin histological analysis

Skin samples from four animals per experimental group (group 1: irradiated and vehicle treated; group 2: irradiated and EUK-207 treated) were harvested at 30 and 90 days after irradiation, fixed in 4% formaldehyde and embedded in paraffin. Tissue sections were stained with hematoxylin and eosin. Epidermal thickness was determined by measuring the epidermal layer and dermal thickness was determined by measuring the dermis from dermo-epidermal junction to the top of fatty layer three times in three consecutive optical fields in each skin sample using Scion image analysis software (National Institutes of Health). The number of hair follicles was determined by manually counting the hair follicles in three consecutive optical fields.

Total RNA extraction and reverse transcription

Skin samples from five animals per experimental group (group 1: irradiated and vehicle-treated; group 2: irradiated and EUK-207 treated; group 3: sham- irradiated and vehicle treated) were harvested at 30 days after irradiation. Samples were washed in ice-cold phosphate-buffered saline (Life Technologies, Carlsbad, CA) and immediately immersed in RNA Later (Life Technologies). The total RNA was prepared using RNeasy Fibrous tissue Mini Kit (Life Technologies), the RNA concentration was determined by 260:280 nm absorbance ratios, equal amounts of RNA from each sample in the experimental group were pooled and cDNA was synthesized from 1 μm of total RNA.

Microarray analysis of skin samples

To determine the relative expression of genes associated with oxidative stress, quantitative real time RT-PCR analysis was performed with RT^2 first strand cDNA kit (SABiosciences, Frederick, MD) and Rat Oxidative Stress and Antioxidant Defense RT^2 Profiler™ PCR Array (SABiosciences). The samples were diluted in qPCR master mix and pipetted into 96-well array plates to evaluate expression of 84 oxidative stress related genes. RT-PCR was performed in technical duplicates using Applied Biosystems Step One Plus Real-Time PCR Systems (Applied Biosystems, Carlsbad, CA). Quality controls included in each plate confirmed the lack of DNA contamination and tested for successful PCR performance. For data analysis of PCR, the ΔΔCt method was used with algorithms provided by the manufacturer. Fold changes were then calculated and expressed as log-normalized ratios of values from irradiated versus sham-irradiated tissues or irradiated and EUK-207 treated tissues.

Detection of carbonylated proteins in the skin extracts

To detect the carbonyl groups we employed the Oxyblot™ Oxidized Protein Detection Kit (Chemicon International, Temecula, CA), which detects proteins containing 2,4-dinitrophenol (DNP)-derivatized carbonyl groups by immunoblotting. Skin tissue samples were rapidly frozen in liquid nitrogen. Equal amounts (100 mg) of skin tissue were each

homogenized in ice cold 20 mM Tris HCl buffer containing Protease Inhibitor Cocktail (Sigma-Aldrich Corp., St. Louis, MO), incubated for 30 minutes on ice, and then centrifuged at 10,000 RPM for 20 min at 4°C. The supernatant was collected and protein concentration was determined by the Bio-Rad Protein Assay (Bio-Rad Laboratories, Hercules, CA). The 20 ug aliquots of protein extracts were analyzed according the manufacturer's protocol. Following the Oxyblot procedure, the PVDF membrane was stripped and probed with specific anti-β actin antibodies (Santa Cruz Biotechnology Inc., Santa Cruz, CA). The protein bands on the membrane were detected using a chemiluminescence detection kit (Pierce, Rockford, IL). The intensity of the bands was quantified by densitometric analysis with NIH image J 1.43 and expressed as density relative to β actin loading control.

Detection of DNA oxidation products

To further confirm the occurrence of oxidative stress in the irradiated skin at 90 days after irradiation, we evaluated DNA oxidation using immunohistochemistry. The paraffin embedded skin sections, were deparaffinated rehydrated and treated with sodium citrate buffer (10 mM sodium citrate, 0.05% Tween 20, pH 6.0), for 10 minutes at 95°C. After washing, samples were incubated with mouse anti-8-hydroxyguanosine IgG (Abcam Inc., Cambridge, MA) overnight at 4°C after biotinylation and a blocking procedure, which followed the manufacturer's protocol (Vector Laboratories Inc., Burlingame, CA). Mouse IgG2a (Abcam Inc.) served as an isotype control. After development with diaminobenzidine, the sections were counterstained with hematoxylin, coded and evaluated under a light microscope. Five consecutive images from each slide and the pixels corresponding to the stained region were measured using the NIH Image J program 1.43.

Blood vessel density

The skin and wound edge samples were embedded in OCT compound (Sakura, Japan) for immunofluorescence studies. Six-micron skin sections were incubated with anti-CD31 IgG (BD Biosciences, San Jose, CA) overnight at 4°C. The mouse IgG2a (Abcam Inc.) served as a negative control. The blood vessels were detected by FITC-conjugated goat F (ab') $_2$ anti-mouse IgG (Santa Cruz Biotechnology Inc.). The slides were coded and evaluated under a fluorescent microscope. Blood vessels in five consecutive images from each slide were counted from four animals per experimental group.

Statistical analysis

For radiation dermatitis scores, differences in treatment group medians were assessed using a Wilcoxon-Mann-Whitney Rank Sum test. For histological analysis all values were expressed as mean ± SD and differences assessed using a two tailed Student's t-test. For all other data, differences among treatment group means were assessed using a one-way ANOVA followed by a Student-Newman-Keuls post hoc test and data expressed as mean ± SD. For all analyses, $p < 0.05$ was considered to be statistically significant.

Acknowledgments

This work was funded by a pilot grant (ZL) under AI067734 (JEM) and Froedtert Hospital Skin Cancer Grant (ZL). Development of EUK-207 was funded in part by GM57770 (SRD).

References

Aykin-Burns N, Slane BG, Liu AT, et al. Sensitivity to Low-Dose/Low-LET Ionizing Radiation in Mammalian Cells Harboring Mutations in Succinate Dehydrogenase Subunit C is Governed by Mitochondria-Derived Reactive Oxygen Species. Radiat Res. 2011; 175:150–158. [PubMed: 21268708]

Clausen A, Doctrow S, Baudry M. Prevention of cognitive deficits and brain oxidative stress with superoxide dismutase/catalase mimetics in aged mice. Neurobiol Aging (online 2008). 2010; 31:425–433.

Cox AG, Winterbourn CC, Hampton MB. Mitochondrial peroxiredoxin involvement in antioxidant defence and redox signalling. Biochem J. 2010; 425:313–325.

Demianenko IA, Vasilieva TV, Domnina LV, et al. Novel mitochondria-targeted antioxidants,"Skulachev-ion" derivatives, accelerate dermal wound healing in animals. Biochemistry (Mosc). 2010; 75:274–280. [PubMed: 20370605]

Doctrow S, Liesa M, Melov S, et al. Salen Mn complexes are superoxide dismutase/catalase mimetics that protect the mitochondria. Curr Inorg Chem. 2012 in press.

Doctrow, SR.; Adinolfi, C.; Baudry, M., et al. Salen manganese complexes, combined superoxide dismutase/catalase mimetics demonstrate potential for treating neurodegenerative and other age-associated diseases. chapter 71. In: Rodriguez, H.; Cutler, R., editors. Oxidative Stress and Aging: Advances in Basic Science, Diagnostics, and Intervention. Vol. Vol. I. Singapore, London, NJ: World Scientific Publishing Company; 2003. p. 1324-1342.

Doctrow, SR.; Baudry, M.; Huffman, K., et al. Salen Mn complexes: multifunctional catalytic antioxidants protective in models for neurodegenerative disease and aging. In: Sessler SRD, JL.; McMurry, TJ.; Lippard, SJ., editors. Medicinal Inorganic Chemistry. New York: American Chemical Society and Oxford University Press; 2005. p. 319-347.

Doctrow, SR.; Huffman, K.; Marcus, CB., et al. Salen-manganese complexes: combined superoxide dismutase/catalase mimics with broad pharmacological efficacy. In: Sies, H., editor. Antioxidants in Disease Mechanisms and Therapeutic Strategies. Vol. Vol. 38. New York: Academic Press; 1997. p. 247-270.

Doctrow SR, Huffman K, Marcus CB, et al. Salen-manganese complexes as catalytic scavengers of hydrogen peroxide and cytoprotective agents: structure-activity relationship studies. J Med Chem. 2002; 45:4549–4558. [PubMed: 12238934]

Epperly MW, Wegner R, Kanai AJ, et al. Effects of MnSOD-plasmid liposome gene therapy on antioxidant levels in irradiated murine oral cavity orthotopic tumors. Radiat Res. 2007; 167:289–297. [PubMed: 17316075]

Gao F, Fish BL, Szabo A, et al. Short-term treatment with a SOD/catalase mimetic, EUK-207, mitigates pneumonitis and fibrosis after single-dose total body or whole-thoracic irradiation. Radiat Res. 2012 in press.

Gonzalez PK, Zhuang J, Doctrow SR, et al. EUK-8, a synthetic superoxide dismutase and catalase mimetic, ameliorates acute lung injury in endotoxemic swine. J Pharmacol Exp Ther. 1995; 275:798–806. [PubMed: 7473169]

Greenberger JS, Epperly MW. Radioprotective antioxidant gene therapy: potential mechanisms of action. Gene Therapy and Molec Biol. 2004; 8:31–44.

Greenberger JS, Epperly MW. Review. Antioxidant gene therapeutic approaches to normal tissue radioprotection and tumor radiosensitization. In Vivo. 2007; 21:141–146. [PubMed: 17436562]

Gurtner GC, Werner S, Barrandon Y, Longaker MT. Wound repair and regeneration. Nature. 2008; 453:314–321. [PubMed: 18480812]

Halliwell, B.; Gutteridge, JMC. Free Radicals in Biology and Medicine. 4th edn.. Oxford: Oxford University Press; 2007. p. 704

Handy DE, Lubos E, Yang Y, et al. Glutathione peroxidase-1 regulates mitochondrial function to modulate redox-dependent cellular responses. J Biol Chem. 2009; 284:11913–11921. [PubMed: 19254950]

Hinerfeld D, Traini MD, Weinberger RP, et al. Endogenous mitochondrial oxidative stress: neurodegeneration, proteomic analysis, specific respiratory chain defects, and efficacious

antioxidant therapy in superoxide dismutase 2 null mice. J Neurochem. 2004; 88:657–667. [PubMed: 14720215]

Jiang J, Stoyanovsky DA, Belikova NA, et al. A mitochondria-targeted triphenylphosphonium-conjugated nitroxide functions as a radioprotector/mitigator. Radiat Res. 2009; 172:706–717. [PubMed: 19929417]

Jourdan MM, Lopez A, Olasz EB, et al. Laminin 332 Deposition is Diminished in Irradiated Skin in an Animal Model of Combined Radiation and Wound Skin Injury. Radiat Res. 2011; 176:636–648. [PubMed: 21854211]

Jung C, Rong Y, Doctrow S, et al. Synthetic superoxide dismutase/catalase mimetics reduce oxidative stress and prolong survival in a mouse amyotrophic lateral sclerosis model. Neurosci Lett. 2001; 304:157–160. [PubMed: 11343826]

Kumin A, Schafer M, Epp N, et al. Peroxiredoxin 6 is required for blood vessel integrity in wounded skin. J. Cell Biol. 2007; 179:747–760. [PubMed: 18025307]

Levine RL. Carbonyl modified proteins in cellular regulation, aging, and disease. Free Radic Biol Med. 2002; 32:790–796. [PubMed: 11978480]

Levine RL, Williams JA, Stadtman ER, et al. Carbonyl assays for determination of oxidatively modified proteins. Methods Enzymol. 1994; 233:346–357. [PubMed: 8015469]

Liesa M, Luptak I, Qin F, et al. Mitochondrial transporter ATP binding cassette mitochondrial erythroid is a novel gene required for cardiac recovery after ischemia/reperfusion. Circulation. 2011; 124:806–813. [PubMed: 21788586]

Liu R, Liu IY, Bi X, et al. Reversal of age-related learning deficits and brain oxidative stress in mice with superoxide dismutase/catalase mimetics. Proc Natl Acad Sci U S A. 2003; 100:8526–8531. [PubMed: 12815103]

Liu X, Liu JZ, Zhang E, et al. Impaired wound healing after local soft x-ray irradiation in rat skin: time course study of pathology, proliferation, cell cycle, and apoptosis. J Trauma. 2005; 59:682–690. [PubMed: 16361913]

Luo JD, Wang YY, Fu WL, et al. Gene therapy of endothelial nitric oxide synthase and manganese superoxide dismutase restores delayed wound healing in type 1 diabetic mice. Circulation. 2004; 110:2484–2493. [PubMed: 15262829]

Mahmood J, Jelveh S, Calveley V, et al. Mitigation of radiation-induced lung injury by genistein and EUK-207. Int J Radiat Biol. 2011; 87:889–901. [PubMed: 21675818]

Melov S, Doctrow SR, Schneider JA, et al. Lifespan extension and rescue of spongiform encephalopathy in superoxide dismutase 2 nullizygous mice treated with superoxide dismutase-catalase mimetics. J Neurosci. 2001; 21:8348–8353. [PubMed: 11606622]

Mettler FA Jr, Gus'kova AK, Gusev I. Health effects in those with acute radiation sickness from the Chernobyl accident. Health Phys. 2007; 93:462–469. [PubMed: 18049222]

Murphy MP, Smith RA. Targeting antioxidants to mitochondria by conjugation to lipophilic cations. Annu Rev Pharmacol Toxicol. 2007; 47:629–656. [PubMed: 17014364]

Peng J, Stevenson FF, Doctrow SR, et al. Superoxide dismutase/catalase mimetics are neuroprotective against selective paraquat-mediated dopaminergic neuron death in the substantial nigra: implications for Parkinson disease. J Biol Chem. 2005; 280:29194–29198. [PubMed: 15946937]

Peter RU. Cutaneous radiation syndrome in multi-organ failure. BJR Suppl. 2005; 27:180–184.

Riedel F, Philipp K, Sadick H, et al. Immunohistochemical analysis of radiationinduced non-healing dermal wounds of the head and neck. In Vivo. 2005; 19:343–350. [PubMed: 15796196]

Robbins ME, Zhao W. Chronic oxidative stress and radiation-induced late normal tissue injury: a review. Int J Radiat Biol. 2004; 80:251–259. [PubMed: 15204702]

Rong Y, Doctrow SR, Tocco G, et al. EUK-134, a synthetic superoxide dismutase and catalase mimetic, prevents oxidative stress and attenuates kainate-induced neuropathology. Proc Natl Acad Sci U S A. 1999; 96:9897–9902. [PubMed: 10449791]

Rosenthal RA, Huffman K, Fisette L, et al. Orally available Mn porphyrins with superoxide dismutase and catalase activities. J. Biol. Inorg. Chem. 2009; 14:979–991. [PubMed: 19504132]

Rosenthal RA, Fish B, Hill RP, et al. Salen Mn complexes mitigate radiation injury in normal tissues. Anticancer Agents Med Chem. 2011; 11:359–372. [PubMed: 21453241]

Roy S, Khanna S, Nallu K, et al. Dermal wound healing is subject to redox control. Mol Ther. 2006; 13:211–220. [PubMed: 16126008]

Ryan JL. Ionizing radiation: the good, the bad, the ugly. J Invest Dermatol. 2012; 132:985–993. [PubMed: 22217743]

Schwentker A, Evans SM, Partington M, et al. A model of wound healing in chronically radiation-damaged rat skin. Cancer Lett. 1998; 128:71–78. [PubMed: 9652795]

Sen CK, Roy S. Redox signals in wound healing. Biochim Biophys Acta. 2008; 1780:1348–1361. [PubMed: 18249195]

Sharpe MA, Ollosson R, Stewart VC, et al. Oxidation of nitric oxide by oxomanganese salen complexes: a new mechanism for cellular protection by superoxide dismutase/catalase mimetics. Biochem J. 2002; 366:97–107. [PubMed: 11994046]

Tie L, Yang HQ, An Y, Liu, et al. Ganoderma Lucidum polysaccharide accelerates refractory wound healing by inhibition of mitochondrial oxidative stress in Type 1 diabetes. Cell. Physiol. Biochem. 2012; 29:583–594. [PubMed: 22508065]

Ukai Y, Kishimoto T, Ohdate T, et al. Glutathione peroxidase 2 in Saccharomyces cerevisiae is distributed in mitochondria and involved in sporulation. Bioch. Biophys. Res. Comm. 2011; 411:580–585.

Ushio-Fukai M, Alexander RW. Reactive oxygen species as mediators of angiogenesis signaling: role of NAD(P)H oxidase. Mol Cell Biochem. 2004; 264:85–97. [PubMed: 15544038]

Wang J, Boerma M, Fu Q, et al. Radiation responses in skin and connective tissues: effect on wound healing and surgical outcome. Hernia. 2006; 10:502–506. [PubMed: 17047884]

Wehr NB, Levine R. Quantitation of protein carbonylation. Free Radic Biol Med. 2012 in press.

West XZ, Malinin NL, Merkulova AA, et al. Oxidative stress induces angiogenesis by activating TLR2 with novel endogenous ligands. Nature. 2010; 467:972–976. [PubMed: 20927103]

Wong GH, Kaspar RL, Vehar G. Tumor necrosis factor and lymphotoxin: protection against oxidative stress through induction of MnSOD. EXS. 1996; 77:321–333. [PubMed: 8856983]

Yan S, Brown SL, Kolozsvary A, et al. Mitigation of radiation-induced skin injury by AAV2-mediated MnSOD gene therapy. J Gene Med. 2008; 10:1012–1018. [PubMed: 18613255]

Zhang HJ, Doctrow SR, Xu L, et al. Redox modulation of the liver with chronic antioxidant enzyme mimetic treatment prevents age-related oxidative damage associated with environmental stress. Faseb J. 2004; 18:1547–1549. [PubMed: 15319374]

Zhang S, Song C, Zhou J, et al. Amelioration of radiation-induced skin injury by adenovirus-mediated heme oxygenase-1 (HO-1) overexpression in rats. Radiat Oncol. 2012; 7:4. [PubMed: 22247972]

Zhao W, Diz DI, Robbins ME. Oxidative damage pathways in relation to normal tissue injury. Br J Radiol. 2007; 80(Spec No 1):S23–S31. [PubMed: 17704323]

Zhao W, Robbins ME. Inflammation and chronic oxidative stress in radiationinduced late normal tissue injury: therapeutic implications. Curr Med Chem. 2009; 16:130–143. [PubMed: 19149566]

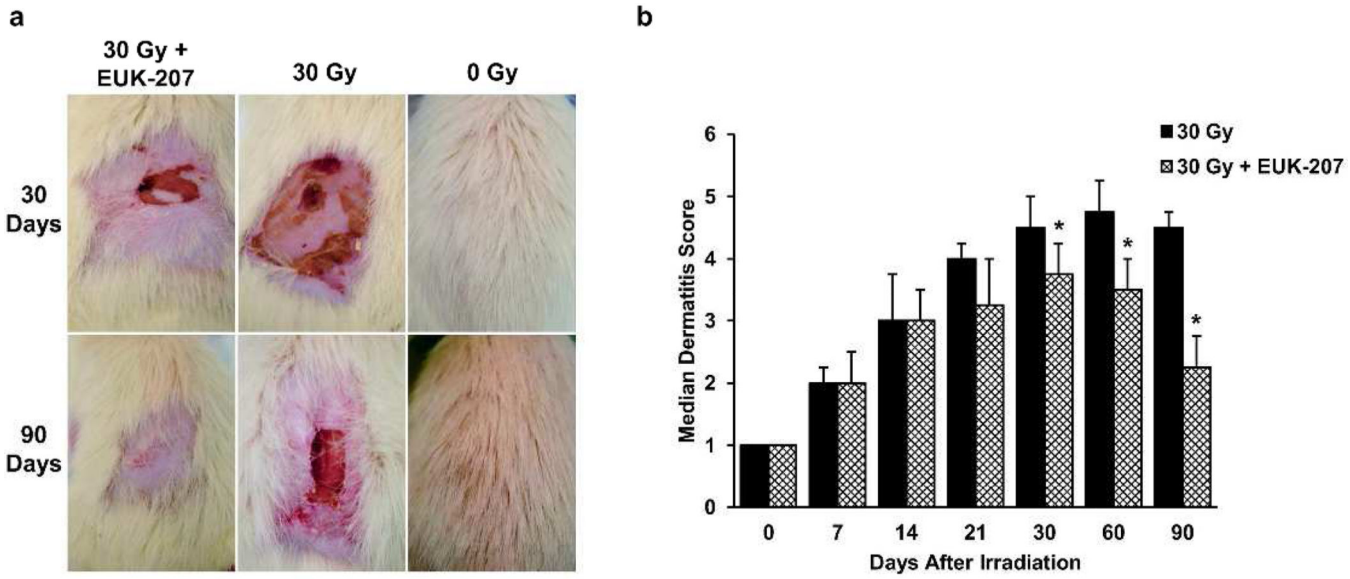

Figure 1. Mitigation of radiation dermatitis by EUK-207

(**a**) Macroscopic comparison of radiation dermatitis in representative rats with or without EUK-207 treatment at indicated radiation dose and time points. (**b**) Time-course of skin injury scores; each point represents data from 8 animals. The bars show the median values and the error bars are the ranges. All scores beyond 21 days (*) are significantly reduced versus age-matched vehicle treated animals ($p<0.01$). Severe radiation dermatitis persists in the vehicle-treated rats at 90 days and the puncture wounds are not healed. Dermatitis is still evident in EUK-207 treated rats at 30 days but puncture wounds were partially to fully closed by that time point, with complete wound healing, indicated by smooth circular scar, in the group by day 40 (35 ± 4 days).

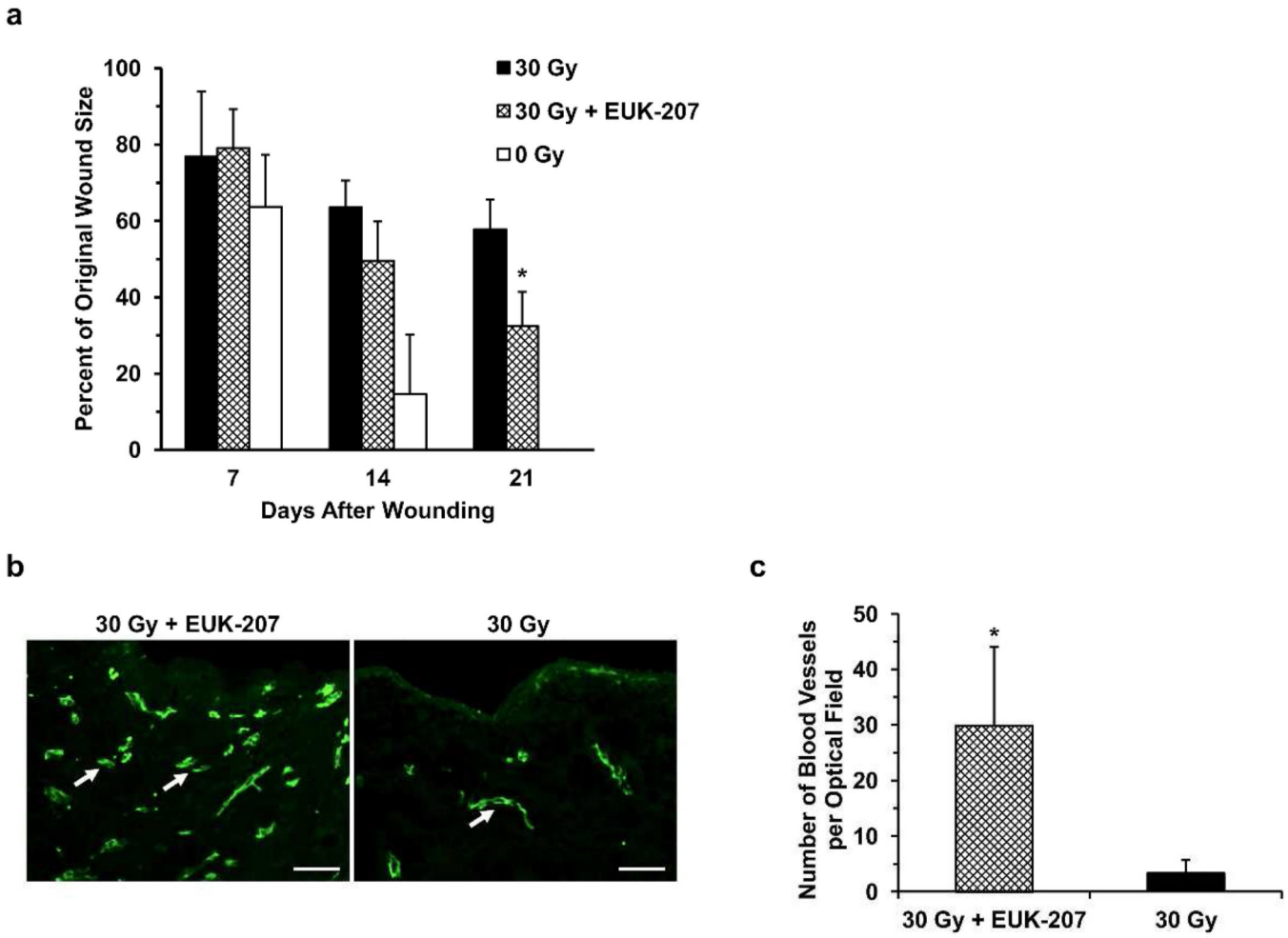

Figure 2. Wound closure and evaluation of blood vessels in irradiated skin

(**a**) The columns represent mean values, bars ± SD, and the asterisk denotes significantly greater wound closure in EUK-207 treated, versus vehicle-treated, irradiated animals. Each time point represents data from 7 animals. (**b**) Representative fluorescence micrograph demonstrating a number of CD31 positive vessels in skin samples taken from the wound edge at the 30 day post-irradiation time point. (**c**) The quantification of CD31 positive vessels in irradiated and EUK-207 or vehicle treated wound edge skin. (*) represents *p*-values < 0.006. Bar = 100 μm.

a

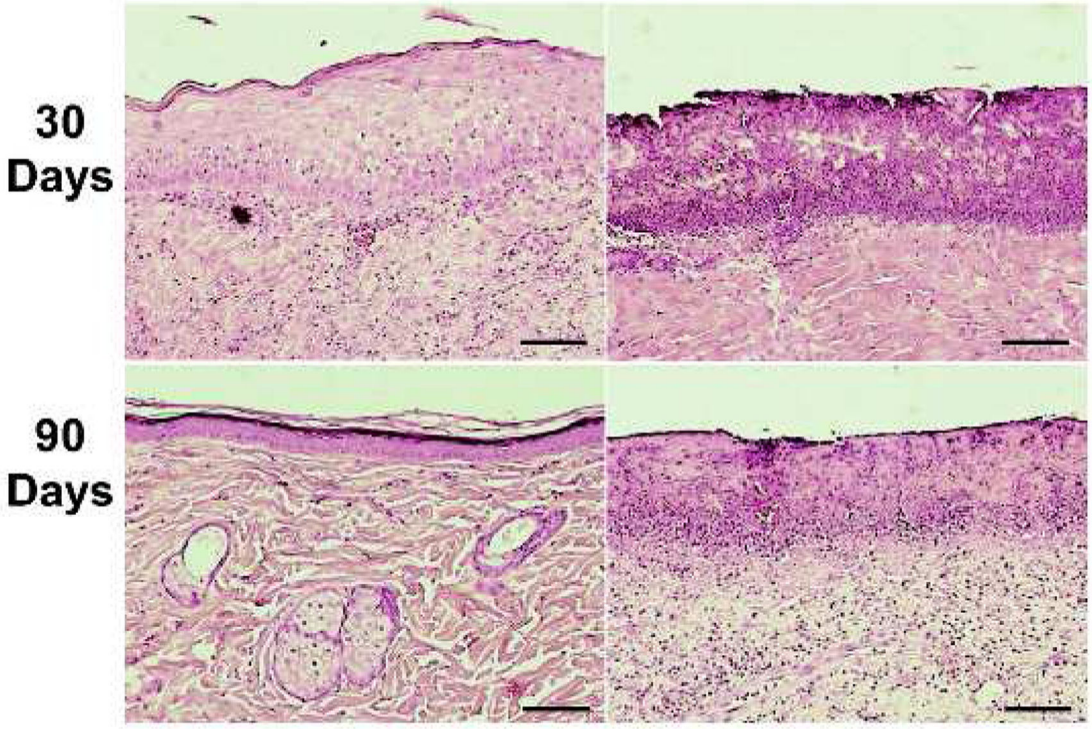

b

Experimental Condition	Days After Irradiation	Dermal Thickness	Epidermal Thickness	Hair Follicles
30 Gy	30	608.4 ± 77.9	0 ± 0	0 ± 0
30 Gy + EUK-207	30	509.9 ± 75.2 *	31.6 ± 30.0 *	3.8 ± 3.9
30 Gy	90	711.7 ± 103.7	14.0 ± 14.6	1.3 ± 1.9
30 Gy + EUK-207	90	566.4 ± 70.1 *	21.7 ± 5.1	6.2 ± 3.2 **

Figure 3. Histological evaluation of irradiated skin

(**a**) Hematoxylin and eosin staining of irradiated skin from rats with or without EUK-207 treatment at indicated time points after irradiation. (**b**) Evaluation of epidermal and dermal thickness and number of hair follicles in skin of experimental and control animals at 30 and 90 days after irradiation. (*) represents *p*-values < 0.005. (**) represents *p*-value < 0.03. Bar = 200 μm.

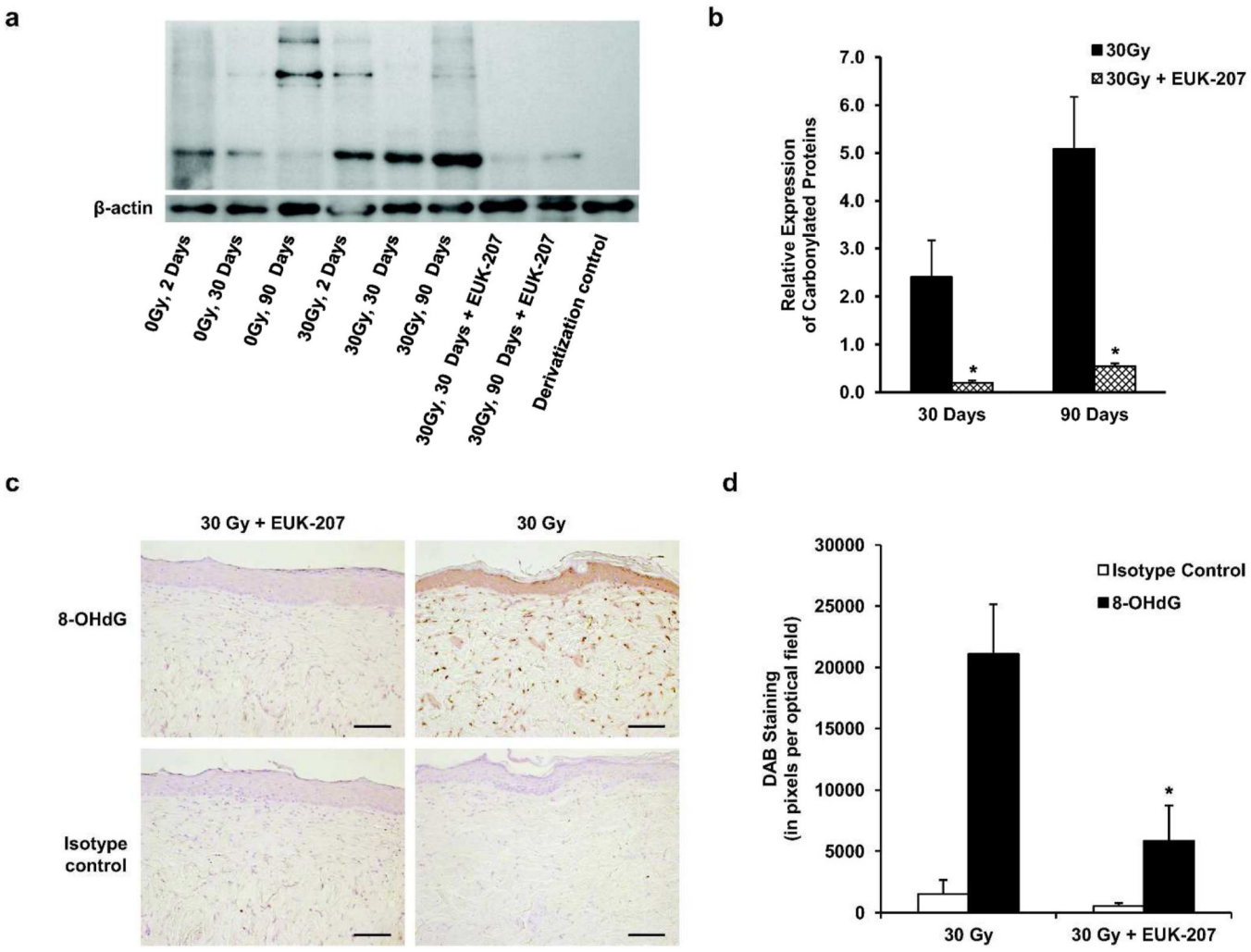

Figure 4. Detection of oxidative stress markers in irradiated skin

(**a**) Representative Western blot of carbonylated proteins at different time points. (**b**) Densitometric evaluation of carbonylated proteins. Asterisks indicate statistically significant differences (vs. 30 Gy) ($p<0.05$). All experimental conditions were run in triplicate. (**c**) Immunohistochemical staining was used to locate the DNA oxidation product 8-OHdG in irradiated and EUK-207 or vehicle treated skin, 90 days following irradiation. (**d**) The intensity of 8-OHdG staining was quantified in the skin, as described in Methods. Asterisk labels statistically-significant decreased staining in EUK-207 treated irradiated animals ($p<0.001$ versus vehicle-treated irradiated animals). Bar = 200 μm.

Table 1
Evaluation of oxidative stress-related gene expression in irradiated skin

(**a**) The list of differentially expressed genes in irradiated skin at 30 days following irradiation, from rats treated with (**a**) vehicle or (**b**) EUK-207 as described in Methods.

a Differentially expressed genes in irradiated and vehicle treated skin

Unigene ID	Reference Sequence	Gene symbol	Gene Name	Fold Change
Rn.162331	XM_344156	Ncf2	Neutrophil cytosolic factor 2	**70.07**
Rn.3928	NM_144737	Fmo2	Flavin containing monooxygenase 2	**29.61**
Rn.38575	NM_053734	Ncf1	Neutrophil cytosolic factor 1	**19.20**
Rn.10488	NM_017051	Sod2	Superoxide dismutase 2, mitochondrial	**17.54**
Rn.32351	NM_138828	Apoe	Apolipoprotein E	**12.34**
Rn.2710	NM_031140	Vim	Vimentin	**10.35**
Rn.55542	NM_024141	Duox2	Dual oxidase 2	**10.02**
Rn.137930	XM_225268	RGD1560658	Similar to serine (or cysteine) proteinase inhibitor, clade B, member 1b	**7.58**
Rn.40511	NM_021588	Mb	Myoglobin	**6.23**
Rn.27588	XM_236702	Xirp1	Xin actin-binding repeat containing 1	**5.70**
Rn.2944	NM_053610	Prdx5	Peroxiredoxin 5	**4.50**
Rn.11323	NM_030826	Gpx1	Glutathione peroxidase 1	**4.42**
Rn.19721	NM_053906	Gsr	Glutathione reductase	**3.61**
Rn.105938	NM_130744	Cygb	Cytoglobin	**3.40**
Rn.11234	NM_017000	Nqo1	NAD(P)H dehydrogenase, quinone 1	**3.01**
Rn.12469	XM_216403	Xpa	Xeroderma pigmentosum, complementation group A	**−3.03**
Rn.3503	NM_183403	Gpx2	Glutathione peroxidase 2	**−3.80**
Rn.25565	XM_214130	Zmynd17	Zinc finger, MYND-type containing 17	**−3.81**
Rn.47782	XM_220830	Mpo	Myeloperoxidase	**−4.17**
Rn.1023	NM_139192	Scd1	Stearoyl-Coenzyme A desaturase 1	**−5.18**
Rn.9470	XM_216452	Dhcr24	24-dehydrocholesterol reductase	**−14.96**

b Differentially expressed genes in irradiated and EUK-207 treated skin

Unigene ID	Reference Sequence	Gene Symbol	Gene Name	Fold Change
Rn.42	NM_053576	Prdx6	Peroxiredoxin 6	**3.21**
Rn.107334	NM_013096	Hba-a2	Hemoglobin alpha, adult chain 2	**3.31**
Rn.3503	NM_183403	Gpx2	Glutathione peroxidase 2	**3.50**